SOPHION BIOSCIENCE

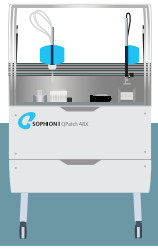

Application Report

hiPSC-derived cardiomyocytes - $Na_V1.5$ compound screening on QPatch® II

Medium-throughput compound screening of $Na_V1.5$ endogenously expressed in hiPSC-cardiomyocytes using automated patch clamp systems

Summary

The $Na_V1.5$ channel is critical in maintaining the physiological electrical function in cardiomyocytes, as it is the heart's main depolarising current. Here we focus on the $Na_V1.5$ channel in human-induced pluripotent stem cell-derived cardiomyocytes (hiPSC-CMs) as an important target for cardiac-drug and safety screening.

- The hiPSC-CMs $Na_V1.5$ compound screening was performed with assay success rate (quality filters) up to 60% and ~ 20 useful experiments per 48 recording site plate.
- The study demonstrates that it is possible to screen compounds on hiPSC-CMs using the QPatch II.
- The experimental success rate of hiPSC-CMs assays was variable depending on the quality and maturation of the cell population.

Introduction

Ion channels play a fundamental role in regulating various aspects of cardiac physiology, constituting the main therapeutic target for cardiac channelopathies[1]. Indeed, it is well known that the balance between different types of ion channels is essential for maintaining the physiological properties of excitable cells, such as cardiomyocytes (CMs). Automated patch clamp (APC) systems are considered efficient and powerful platforms for investigating channel physiology and channelopathies in different research areas, including the field of cardiac biology[1].

After the introduction of the hiPSCs technology by Yamanaka in 2006[2], the development and usage of hiPSCs in cardiovascular research were rapidly adopted. Indeed, hiPSC-cardiomyocytes (hiPSC-CMs) have proven to be a promising model for researchers since they recapitulate the phenotype of human primary CMs, allowing drug discovery and development[3].

However, hiPSC-CMs differentiation remains challenging, as these cells exhibit an immature phenotype, which is not shared with adult CMs (i.e., depolarized diastolic potential, spontaneous action potential generation/automaticity, and lack of I_{K1})[3].

Moreover, electrophysiological experiments with hiPSC-CMs display large phenotype variability because of the lack of standardized handling methods. For all these reasons, there is an urgency to optimize cell suspension quality and purity and assays, particularly for use on APC systems, to improve hiPSC-CMs performance, consistency, and reproducibility[1, 4].

Important potential applications of hiPSC-CMs are cardiac-drug and safety screening and disease modelling. An interesting target in this context is the $Na_V1.5$ channel, which constitutes the main depolarizing current in the heart, and, thus, is required for normal electric conduction and cell excitability[5]. Moreover, its interplay with other ion channels, such as potassium and calcium channels, is crucial to maintain the physiological electric function[6].

Here we conducted a compound screening on the $Na_V1.5$ channel endogenously expressed in hiPSC-CMs using our APC platform, QPatch II. We tested five different $Na_V1.5$ channel blockers with two different voltage protocols.

The first voltage protocol was constructed according to the CiPA recommendations for cardiac safety, whereas the second voltage protocol was designed to investigate the state-dependent inhibitory effect of the compounds.

Our medium throughput drug screening study demonstrates the feasibility of using hiPSC-CMs for drug screening. Since the combination of different voltage protocols and compound effects on hiPSC-CMs on APC systems is still an underexplored area, this study adds novel knowledge in the field.

Results and discussion

Quality of hiPSC-CMs on QPatch II

hiPSC-CMs quality and maturity are known to be variable from vendor to vendor and batch to batch.

In this study, we worked with two different batches of cells yielding 30 – 60% successful experiments.

Success rate was calculated as the percentage of cells passing the following quality filters: i) Whole-cell Resistance > 200 MΩ; ii) C_{slow} > 4 pF out of a full measurement plate. $Na_V1.5$ channel expression was filtered for baseline current I_{Nav} < -200 pA (Table 1).

Table 1: Assay success rate (whole-cell resistance > 200 MΩ; C_{slow} > 4 pF) and $Na_V1.5$ current expression (baseline current < -200 pA) are listed for two cell populations (Batch #1 and Batch #2). Data are presented as avg ± SD of $N_{QPlates}$.

Cell population	Batch #1	Batch #2
Success rate (%) of 48 measurement sites	31±13	60±3
$Na_V1.5$ current expression (%) of successful sites	73±15	98±3
$N_{QPlates}$	22	2

Here we demonstrate that hiPSC-CMs can be measured on QPatch II with a success rate of up to 60% (based on quality filters) and up to 100% of these having $Na_V1.5$ current expression (Table 1). Table 2 contains data regarding the percentage of useful experiments from two QPlates, obtained in a compound screening setup. The percentage of useful concentration-response experiments was up to 45%, but the data show a high batch to batch variation. Therefore, a compound screening on QPatch II is feasible, but with success rates highly depending on the quality of the hiPSC-CM batches used for the studies.

Comparison between hiPSC-CMs at DIV16-17 and DIV30-31

Maturation stage of hiPSC-CMs may also influence electrophysiological results. Because of this, we compared the channel expression within the same cell population at two different maturation stages; at 16-17 days *in vitro* (DIV) and at 30-31 DIV. The percentage of cells with Na_V current did not seem to increase from DIV16-17 to DIV30-31 (data not shown). However, the quantified current density significantly increased (**** Unpaired t-test; P<0.0001) from DIV16-17 to DIV30-31 (Fig. 1). These results are in agreement with findings showing maturation of hiPSC-CMs toward the adult phenotype during time in culture[7].

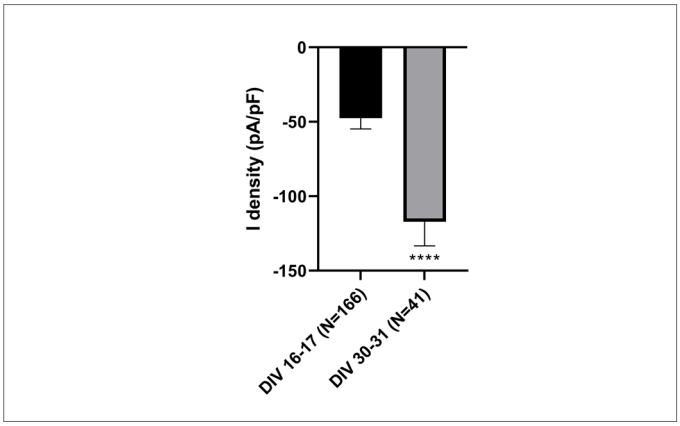

Fig. 1: Current density comparison between DIV16-17 (black) and DIV30-31 (grey) with the CiPA voltage clamp protocol from the pre-compound current (baseline). ****Unpaired t-test; P<0.0001. The values are expressed as average ± SEM.

Next, we evaluated whether the current measured is mediated by channels resistant to nanomolar concentrations of tetrodotoxin (TTX) by performing a TTX concentration-response experiment. TTX was tested only using the CiPA protocol in iPSC-CMs at DIV16-17 (Fig. 2). The IC_{50} value determined was consistent with literature values for the $Na_V1.5$ channel[8, 9].

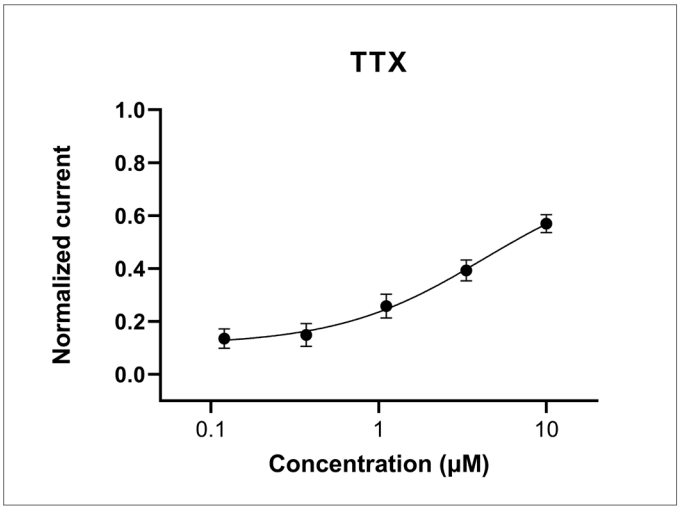

Fig. 2: Concentration-response curve for TTX using the CiPA voltage pulse protocol. The peak currents are normalized to baseline. The data points are presented as average ± SEM of at least eight measurements.

Compound screening

Five different compounds were tested using two voltage protocols (Fig. 9) on hiPSC-CMs at DIV16-17. The following figures show representative current traces in response to the two voltage protocols, using the corresponding block by tetracaine as an example (Fig. 3 and 4).

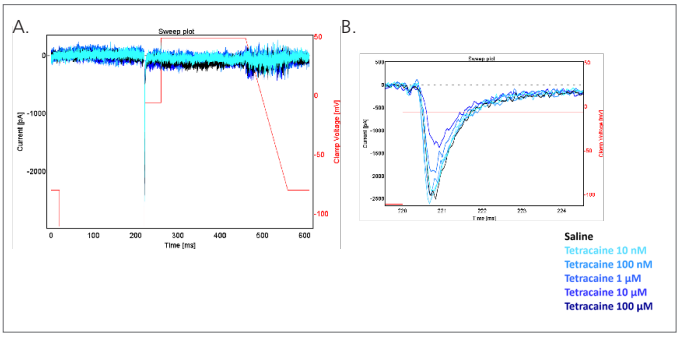

Fig. 3: Representative traces of Na_V current in response to the CiPA voltage protocol. a) View of the entire CiPA protocol; b) Expanded detail of the Na_V peak current [note x-axes for a) and b)]. Both panels show that applying tetracaine at increasing concentrations leads to an increasing Na_V current block. Black: saline; from light blue to dark blue: increasing concentrations of tetracaine from 10 nM to 100 µM.

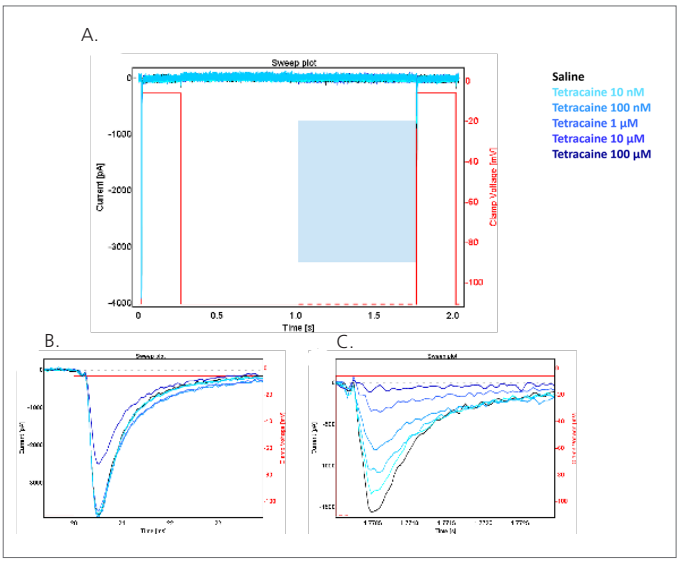

Fig. 4: Representative traces of Na_V current in response to a two-pulse voltage protocol. a) View of the entire two-pulse protocol; b) Expanded detail of Na_V peak current in response to application of the first voltage pulse; c) Expanded detail of Na_V peak current in response to application of the second pulse. As shown in both panels, the application of tetracaine at increasing concentrations leads to increasing Na_V current block, which was fully blocked in the second pulse with the highest concentration of tetracaine (100 µM). Black: saline; from light blue to dark blue: increasing concentrations of tetracaine from 10 nM to 100 µM.

The following five $Na_V1.5$ compound blockers were tested: tetracaine, amitriptyline, amiodarone, flecainide and quinidine. The normalized data were fitted to the Boltzmann equation, and the IC_{50} values for each compound were extracted (Fig. 5-8 and supplementary Fig. S1-S6, table 3). Data from amiodarone, flecainide, and quinidine can be found in the supplemental material. All compounds were applied in a cumulative manner. The average current amplitude ± SEM was calculated and normalized to the pre-compound current (baseline). When the maximal concentration of the compound yield less than 50% of inhibition, the percentage inhibition at the maximal concentration is reported (%Inh[max]).

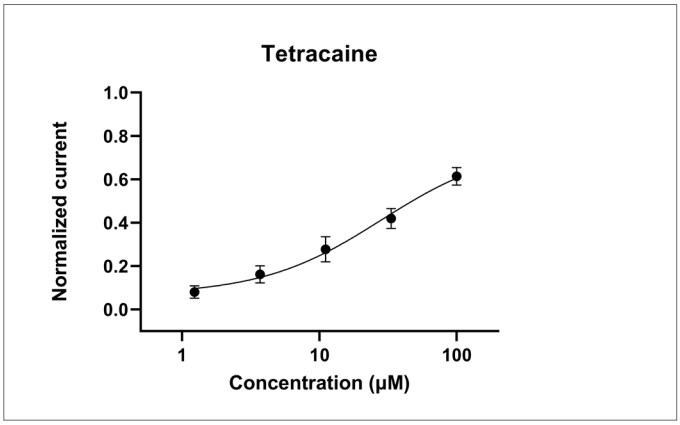

Fig. 5: Concentration-response curve for tetracaine using the CiPA voltage pulse protocol. The peak currents are normalized to baseline. The data points are presented as average ± SEM of at least eight measurements.

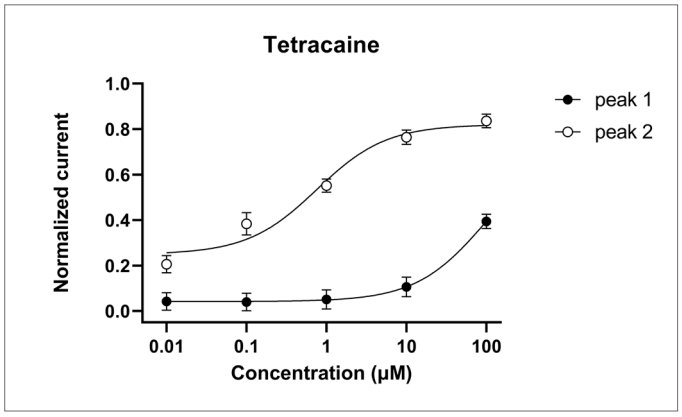

Fig. 6: Concentration-response curve for tetracaine using the two-pulse voltage clamp protocol. The peak currents are normalized to baseline. The data points are presented as average ± SEM of at least eight measurements.

The percentage of useful concentration-response experiments was found to vary between batches of cells. The following table demonstrates how the same experiment with tetracaine performed on two different batches of cells can result in 4 to 44% of useful experiments per measuring plate (Table 2).

Table 2: Example assay success rates of useful experiments for two cell populations (Batch #1 and Batch #2) and the same compound (tetracaine), using the two-pulse voltage protocol. Data are presented as avg ± SD of $N_{QPlates}$.

Cell population	Batch #1	Batch #2
Useful experiments (%) of 48 measurement sites	4.0±0.7	44.8±4.4
$N_{Qplates}$	2	2

As is well-known, IC_{50} values of Na_V channel blocking compounds are influenced by the applied voltage protocol, which makes comparisons between studies difficult[16]. Here we have tested two different voltage protocols, the CiPA suggested by the FDA and the two-pulse protocol testing the closed and inactivated state block. As shown in Table 3, compounds exhibited state-dependent block, as seen from the difference in the IC_{50} values between peaks 1 and 2.

In addition to the differences elucidated from the voltage protocols, compound effects can also be influenced by the cell model. In this case, the hiPSC-CMs model (e.g. endogenous channels, auxiliary subunits, multiple pools of channels, low channel expression levels compared to the overexpressing immortalized cell lines). Although we have not investigated the influence of these specific features of the hiPSC-CMs model, we tested some of the compounds in a HEK cell line stably expressing $Na_V1.5$ on QPatch II. Comparable IC_{50} values were calculated and can be seen in table 3.

Overall, literature IC_{50} values for compounds acting on the $Na_V1.5$ channel on iPSC-CMs are limited. Thus, the comparison of IC_{50} values resulting from our experiments with literature was challenging.

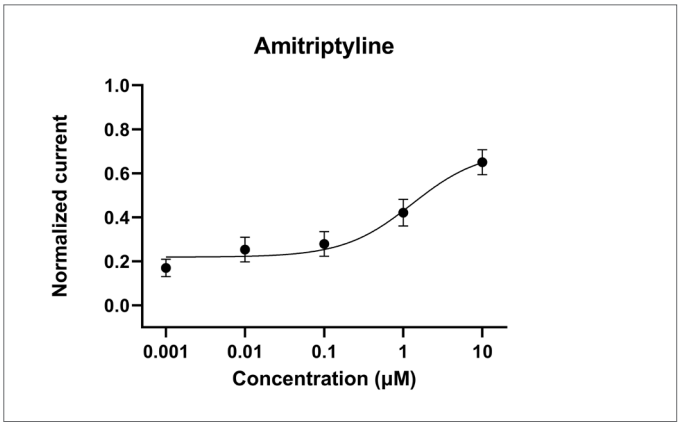

Fig. 7: Concentration-response curve for amitriptyline using the CiPA voltage pulse protocol. The peak currents are normalized to baseline. The data points are presented as average ± SEM of at least eight measurements.

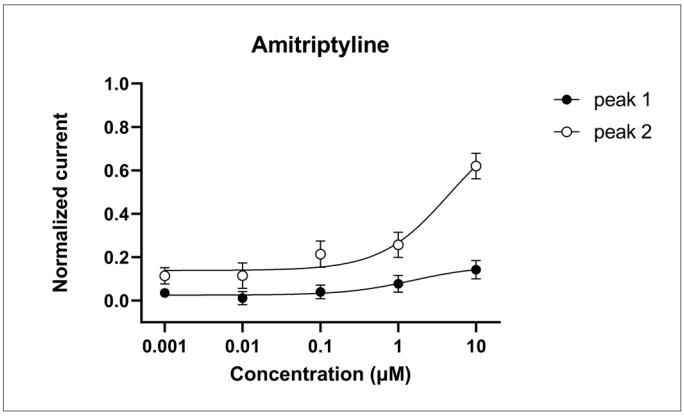

Fig. 8: Concentration-response curve for amitriptyline using the two-pulse voltage clamp protocol. The peak currents are normalized to baseline. The data points are presented as average ± SEM of at least eight measurements.

Table 3: Potency of six reference compounds investigated with two different voltage protocols – see figures 5-8. All values are given in µM or as a percentage of maximal inhibition. #) CiPA voltage protocol; *) two pulse voltage protocol (P1=peak 1, P2=peak 2); °) other voltage protocols.

Cells	iPSC- CMs			HEK cell line			
Compound name	CiPA protocol (µM)	Two pulse protocol (µM)		CiPA protocol (µM)	Two pulse protocol (µM)		Literature IC_{50} (µM)
		1st peak	2nd peak		1st peak	2nd peak	
TTX	4.2	/	/	/	/	/	≥1 [8,9]°
Tetracaine	28.3	%Inh[max]: 38 %	0.8	29.6	%Inh[max]: 40 %	0.8	P1: 22.4, P2: 3 [10]*/ P1: 53.9, P2: 1.3 [12]*
Quinidine	%Inh[max]: 26 %	%Inh[max]: 46 %	12.5	/	/	/	P1: 92.7, P2: 51.4 [10]* / 9.7 [12]°/ 14.6 [13]°/ 46.6 [14]°
Amitriptyline	1.3	%Inh[max]: 10 %	%Inh[max]: 62 %	2.1	%Inh[max]: 10 %	0.8	P1: 13.6, P2: 4 [10]*/ 5.5[14]°
Flecainide	%Inh[max]: 16 %	59.7	6.9	/	/	/	6.2 [13,14]°/ 7.4 (inactivated state) [12]° / 345 (resting block) [12]°/ 8.8 [15]#
Amiodarone	%Inh[max]: 25 %	%Inh[max]: 8 %	%Inh[max]: 36 %	/	/	/	15.9 [13]°

Methods

- Cells were kindly provided by iBET, Oeiras (Portugal) https://www.ibet.pt/
- Cell culture and cell suspension preparation according to internal Sophion methods.
- Compounds (cumulative 5-point dose-response):
  - TTX in 3-fold dilution starting from 10 µM
  - Tetracaine 3-fold dilution starting from 100 µM
  - Quinidine 10-fold dilution starting from 100 µM
  - Amitriptyline 10-fold dilution starting from 10 µM
  - Flecainide 10-fold dilution starting from 100 µM
  - Amiodarone 10-fold dilution starting from 10 µM
- Temperature: default temperature (set at 27 °C using temperature control)

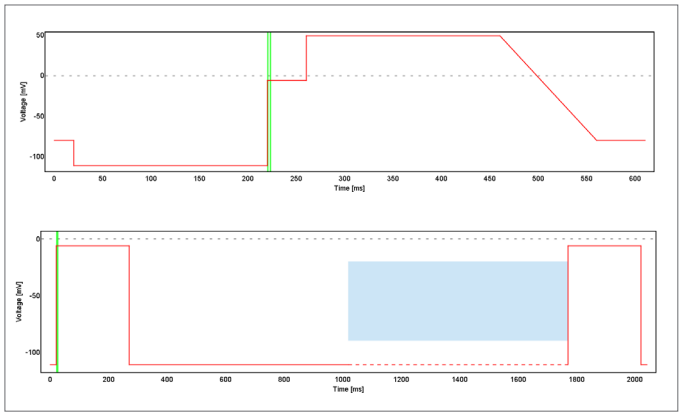

Fig. 9: Voltage protocols used for compound testing.

References

1. Bell, D. C., and Fermini, B. (2021). Use of automated patch clamp in cardiac safety assessment: past, present and future perspectives. Journal of Pharmacological and Toxicological Methods, 110, 107072.
2. Takahashi, K., and Yamanaka, S. (2006). Induction of pluripotent stem cells from mouse embryonic and adult fibroblast cultures by defined factors. cell, 126(4), 663-676.
3. Goversen, B., van der Heyden, M. A., van Veen, T. A., and de Boer, T. P. (2018). The immature electrophysiological phenotype of iPSC-CMs still hampers in vitro drug screening: Special focus on IK1. Pharmacology and therapeutics, 183, 127-136.
4. Di Baldassarre, A., Cimetta, E., Bollini, S., Gaggi, G., and Ghinassi, B. (2018). Human-induced pluripotent stem cell technology and cardiomyocyte generation: Progress and clinical applications. Cells, 7(6), 48.
5. Abriel, H. (2010). Cardiac sodium channel Nav1. 5 and interacting proteins: physiology and pathophysiology. Journal of molecular and cellular cardiology, 48(1), 2-11.
6. Ponce-Balbuena, D., Guerrero-Serna, G., Valdivia, C. R., Caballero, R., Diez-Guerra, F. J., Jiménez-Vázquez, E. N., ... and Jalife, J. (2018). Cardiac Kir2. 1 and Nav1. 5 channels traffic together to the sarcolemma to control excitability. Circulation research, 122(11), 1501-1516.
7. Lundy, S. D., Zhu, W. Z., Regnier, M., and Laflamme, M. A. (2013). Structural and functional maturation of cardiomyocytes derived from human pluripotent stem cells. Stem cells and development, 22(14), 1991-2002.
8. Wang, Y., Mi, J., Lu, K., Lu, Y., and Wang, K. (2015). Comparison of gating properties and use-dependent block of Nav1. 5 and Nav1. 7 channels by anti-arrhythmics mexiletine and lidocaine. PLoS One, 10(6), e0128653.
9. Zimmer, T. (2010). Effects of tetrodotoxin on the mammalian cardiovascular system. Marine Drugs, 8(3), 741-762.
10. ttps://sophion.com/wp-content/uploads/2020/04/JMolBio_2019_poster_final.pdf
11. https://sophion.com/wp-content/uploads/2019/02/Biophysical-pharmacological-profiling-of-multiple-voltage-gated-Nav-channels-on-QPatchII.pdf
12. Ramos, E., and O'leary, M. E. (2004). State-dependent trapping of flecainide in the cardiac sodium channel. The Journal of physiology, 560(1), 37-49.
13. Kramer, J., Obejero-Paz, C. A., Myatt, G., Kuryshev, Y. A., Bruening-Wright, A., Verducci, J. S., and Brown, A. M. (2013). MICE models: superior to the HERG model in predicting Torsade de Pointes. Scientific reports, 3(1), 1-7.
14. Brian T. Donovan; Tania Bakshi; Sarah E. Galbraith; Christopher J. Nixon; Lisa A. Payne; Stan F. Martens (2011). Utility of frozen cell lines in medium throughput electrophysiology screening of hERG and NaV1.5 blockade. , 64(3), 269–276. doi:10.1016/j.vascn.2011.09.002.
15. https://sophion.com/wp-content/uploads/2019/10/SPS-2019-Eurofins-Poster-hNav.pdf
16. England S, de Groot MJ. Subtype-selective targeting of voltage-gated sodium channels. Br J Pharmacol. 2009 Nov;158(6):1413-25. doi: 10.1111/j.1476-5381.2009.00437.x. Epub 2009 Oct 20. PMID: 19845672; PMCID: PMC2795208.

Authors:

Beatrice Badone, Application Scientist

Stefania Karatsiompani, Application Scientist

Supplementary material

We evaluated on hiPSC-CMs five $Na_V1.5$ compound blockers: tetracaine, amiodarone, amitriptyline, flecainide, quinidine, with both the CiPA and the two-pulse voltage clamp protocols. Tetracaine and amiodarone dose response can be found in the main text. All compounds were applied in a cumulative manner.

The average current amplitude ± SEM was calculated and normalized to pre-compound current (baseline). The normalized data were fitted to the Boltzmann equation and the IC_{50} for each compound was extracted. IC_{50} values are are listed in table 3 in the report.

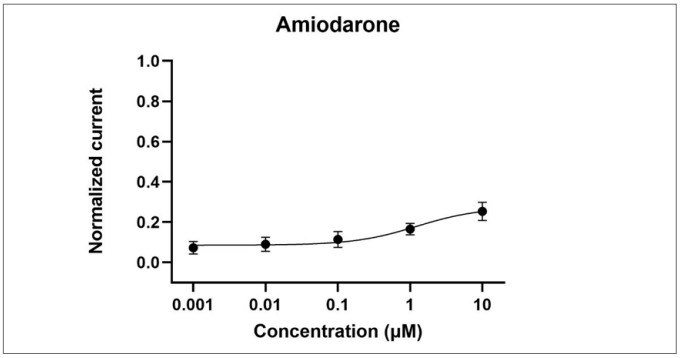

Fig. S1: Dose-response curve for amiodarone using the CiPA voltage pulse protocol. The peak currents are normalized to baseline. The data points are presented as average ± SEM of at least eight measurements.

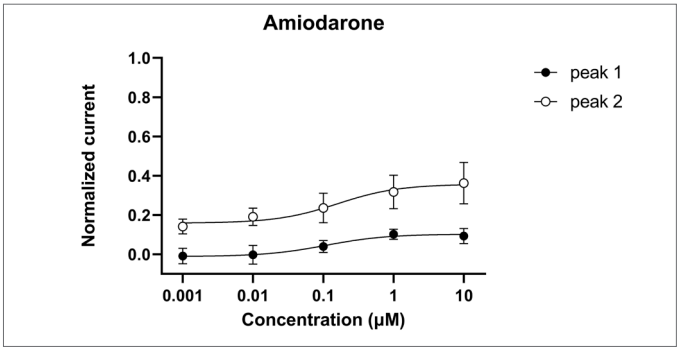

Fig. S2: Dose-response curve for amiodarone using the two-pulse voltage clamp protocol. The peak currents are normalized to baseline. The data points are presented as average ± SEM of at least eight measurements.

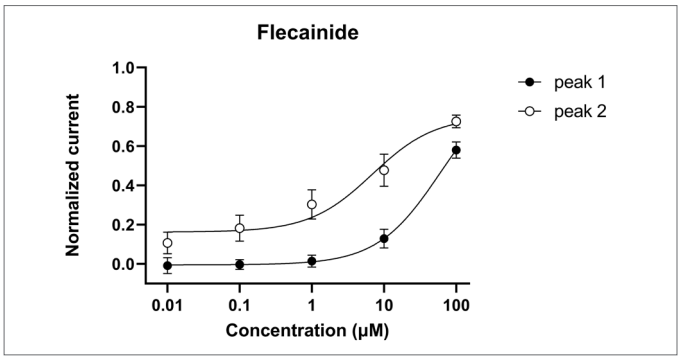

Fig. S4: Dose-response curve for flecainide using the two-pulse voltage clamp protocol. The peak currents are normalized to baseline. The data points are presented as average ± SEM of at least eight measurements.

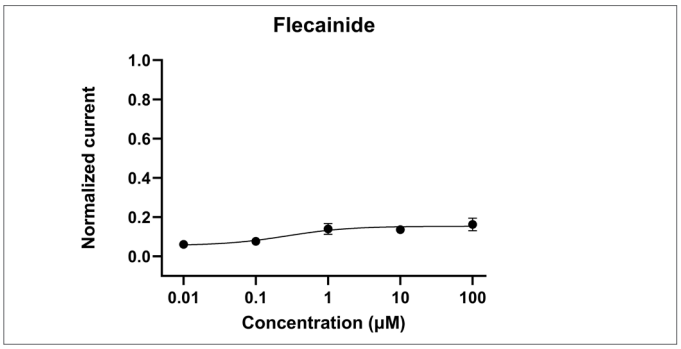

Fig. S3: Dose-response curve for flecainide using the CiPA voltage pulse protocol. The peak currents are normalized on the baseline. The data points are presented as average ± SEM of at least eight measurements.

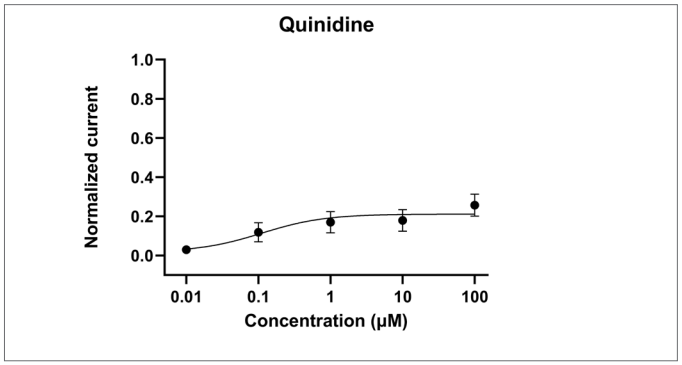

Fig. S5: Dose-response curve for quinidine using the CiPA voltage pulse protocol. The peak currents are normalized to baseline. The data points are presented as average ± SEM of at least eight measurements.

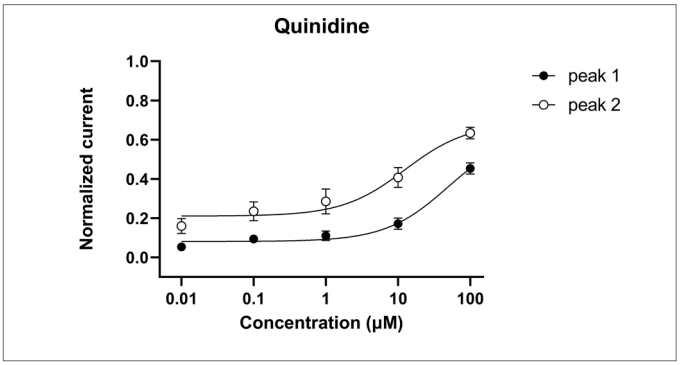

Fig. S6: Dose-response curve for quinidine using the two-pulse voltage clamp protocol. The peak currents are normalized to baseline. The data points are presented as average ± SEM of at least eight measurements.